

Fracture Testing of a Self-Healing Polymer Composite

by E.N. Brown, N.R. Sottos and S.R. White

ABSTRACT—Inspired by biological systems in which damage triggers an autonomic healing response, a polymer composite material that can heal itself when cracked has been developed. In this paper we summarize the self-healing concept for polymeric composite materials and we investigate fracture mechanics issues consequential to the development and optimization of this new class of material. The self-healing material under investigation is an epoxy matrix composite, which incorporates a microencapsulated healing agent that is released upon crack intrusion. Polymerization of the healing agent is triggered by contact with an embedded catalyst. The effects of size and concentration of the catalyst and microcapsules on fracture toughness and healing efficiency are investigated. In all cases, the addition of microcapsules significantly toughens the neat epoxy. Once healed, the self-healing polymer exhibits the ability to recover as much as 90 percent of its virgin fracture toughness.

KEY WORDS—Self-healing, autonomic healing, fracture toughness, microcapsule toughening, tapered double-cantilevered beam, brittle fracture of epoxy

Introduction

Fracture of the skeletal structure in biological systems provides an excellent model for developing a synthetic healing process for structural materials. For a bone to heal, nutrients and undifferentiated stem cells must be delivered to the fracture site and sufficient healing time must elapse.¹ The healing process consists of multiple stages of deposition and assembly of material,² as illustrated in Fig. 1. The network of blood vessels in the bone is ruptured by the fracture event, initiating autonomic healing by delivering the components needed to regenerate the bone.

In recent breakthrough research, White *et al.*³ have developed a self-healing polymer that mimics many of the features of a biological system. The self-healing system, shown schematically in Fig. 2, involves a three-stage healing process, accomplished by incorporating a microencapsulated healing agent and a catalytic chemical trigger in an epoxy matrix. A conclusive demonstration of self-healing was obtained with a healing agent based on the ring-opening metathesis polymerization (ROMP) reaction. Dicyclopenta-

diene (DCPD), a highly stable monomer with excellent shelf life, was encapsulated in microcapsules with a thin shell made of urea-formaldehyde. A small volume fraction of microcapsules was dispersed in a common epoxy resin along with the Grubbs ROMP catalyst, a living catalyst that remains active after triggering the polymerization. The embedded microcapsules were shown to rupture in the presence of a crack and to release the DCPD monomer into the crack plane. Contact with the embedded Grubbs catalyst initiated polymerization of the DCPD and rebonded the crack plane. Crack healing efficiency, η , is defined as the ability of a healed sample to recover fracture toughness⁴

$$\eta = \frac{K_{IC_{healed}}}{K_{IC_{virgin}}}, \quad (1)$$

where $K_{IC_{virgin}}$ is the fracture toughness of the virgin specimen and $K_{IC_{healed}}$ is the fracture toughness of the healed specimen. Fracture test results using the ROMP-based healing system revealed that, on average, 60 percent of the fracture toughness was recovered in the healed samples.

Crack healing phenomena have been discussed in the literature for several types of synthetic materials including glass, concrete, asphalt and a range of polymers.^{4–22} While these previous works have been successful in repairing or sealing cracks, the healing was not self-initiated and required some form of manual intervention (e.g., application of heat, solvents, or healing agents). Others have proposed a tube delivery concept for self-repair of corrosion damage in concrete and cracks in polymers.^{23–25} While conceptually interesting, the introduction of large hollow tubes in a brittle matrix material causes stress concentrations that weaken the material, and beneficial healing may be difficult to realize.²⁵

In contrast, the microcapsule concept developed by White *et al.*³ is particularly elegant and promising for healing brittle, thermosetting polymers. In this paper, we present a comprehensive experimental investigation of the correlative fracture and healing mechanisms of this self-healing system. The effects of microcapsule concentration, catalyst concentration and healing time are studied with a view towards improving healing efficiency.

Experimental Procedure

Using the protocol established by White *et al.*,³ healing efficiency is measured by carefully controlled fracture experiments for both the virgin and the healed materials. These tests utilize a tapered double-cantilever beam (TDCB) geometry, which ensures controlled crack growth along the centerline of the brittle specimen. The TDCB fracture geometry, developed by Mostovoy *et al.*,²⁶ provides a crack length independent measure of fracture toughness

Eric N. Brown is a Doctoral Candidate and Nancy R. Sottos is a Professor, Department of Theoretical and Applied Mechanics and Beckman Institute for Advanced Science and Technology, 216 Talbot Laboratory, 104 South Wright Street Urbana, IL 61801. Scott R. White is a Professor, Department of Aerospace Engineering and Beckman Institute for Advanced Science and Technology, 306 Talbot Laboratory, 104 South Wright Street, Urbana, IL 61801.

Original manuscript submitted: February 26, 2002.

Final manuscript received: August 6, 2002.

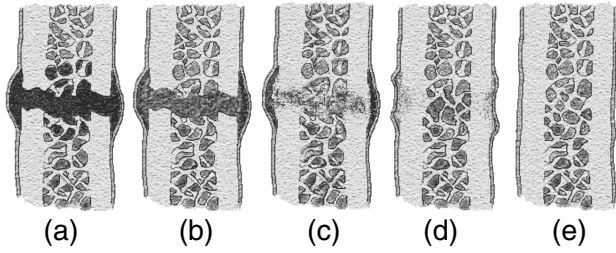


Fig. 1—Healing stages of bone: (a) internal bleeding, forming a fibrin clot; (b) unorganized fiber mesh develops; (c) calcification of the fibrocartilage; (d) calcification converted into fibrous bone; (e) transformation into lamellar bone

$$K_{Ic} = 2P_c \frac{\sqrt{m}}{\beta}, \quad (2)$$

which requires knowledge of only the critical fracture load P_c and geometric terms m and β . The value of β depends on the specimen and crack widths b and b_n , respectively. The value of m is defined by the theoretical relation

$$m = \frac{3a^2}{h(a)^3} + \frac{1}{h(a)}, \quad (3)$$

or determined experimentally by the Irwin-Kies²⁷ method where

$$m = \frac{Eb}{8} \frac{dC}{da}. \quad (4)$$

Young's modulus is given by E , C is the compliance, a is the crack length from the line of loading, and $h(a)$ is the specimen height profile. For the TDCB sample geometry, the healing efficiency (eq (1)) is rewritten as

$$\eta = \frac{P_{C_{healed}}}{P_{C_{virgin}}}. \quad (5)$$

TDCB Specimen

Valid profiles for a TDCB fracture specimen are determined by finding a height profile that, when inserted into eq (3), yields a constant value of m over a desired range of crack lengths. Height profiles that provide an exact solution are complex curves, but are approximated with linear tapers.^{12,26,28,29} In the current work, we adopt a modified version of the TDCB geometry developed and verified by Beres *et al.*²⁸ Relevant dimensions are shown in Fig. 3.

When the taper angle is small, a crack propagating in a brittle material exhibits a propensity to deflect significantly from the centerline. Failure commonly occurs as arm break-off. To ensure fracture follows along the desired path, side grooves are incorporated into the TDCB geometry. The addition of side grooves is valid for the TDCB geometry, as there is no restriction that b and b_n be the same. Stable crack propagation with maximum crack width, b_n , is obtained by selecting a groove with 45° internal angle.³⁰ For this particular geometry, the geometric term β in eq (2) is given by³¹ $\beta = b^{0.61} b_n^{0.39}$.

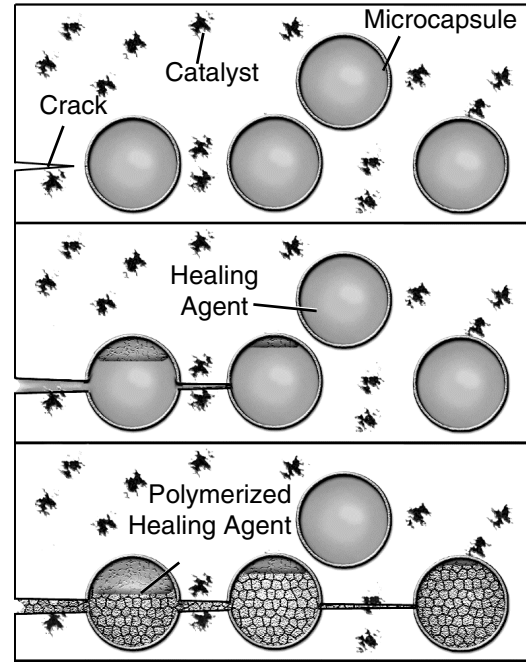


Fig. 2—Self-healing concept for a thermosetting polymer

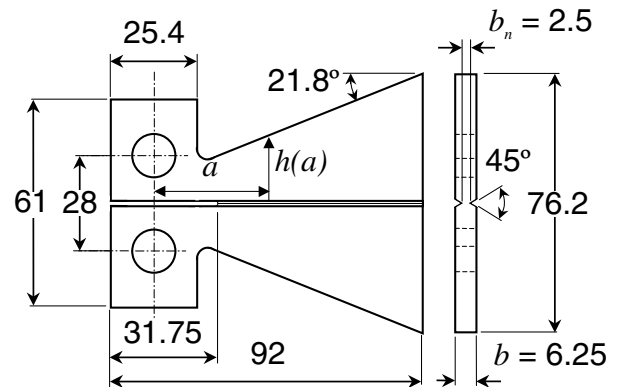


Fig. 3—TDCB geometry (dimensions in mm)

A series of 18 fracture toughness tests was performed on pure epoxy (EPON[®] 828/DETA) TDCB specimens with crack lengths ranging from 20 to 37 mm to determine m from eq (4). A plot of compliance versus crack length was constructed and a linear fit made, extrapolating a constant value of dC/da . The fracture toughness of the neat epoxy and the geometric constant m were measured to be 0.55 MPa $m^{1/2}$ and 0.6 mm^{-1} . This experimental value of m is in excellent agreement with the value predicted by the finite element method (FEM).²⁸ The Young's modulus of the epoxy was measured according to the American Society for Testing and Materials (ASTM) Standard D 638, $E = 3.4 \pm 0.1$ GPa.

Sample Preparation and Test Method

Samples were prepared by mixing EPON[®] 828 epoxy resin with 12 pph Anacmine[®] DETA curing agent. The epoxy

mixture was degassed, poured into a closed silicone rubber mold and cured for 24 h at room temperature, followed by 24 h at 30°C. After curing, a sharp pre-crack was created by gently tapping a razor blade into the molded starter notch in the samples. To facilitate investigation of the effects of the constituents on the self-healing system, varying weight percent of Grubbs catalyst and/or microcapsules were mixed into the resin prior to pouring.

Three types of experiments were conducted: two types of control in addition to the self-healing *in situ* tests. The first type of control, referred to as reference samples, consisted of epoxy without embedded catalyst. Reference samples with a range of microcapsule concentrations were investigated; however, the content of the microcapsules in these samples was not utilized for the healing process. Reference samples were tested to failure and then manually healed by injection of DCPD monomer that was pre-mixed with catalyst. Reference tests removed the variables associated with DCPD delivery and the embedding of Grubbs catalyst. The second control, referred to as self-activated samples, consisted of epoxy with embedded catalyst but no microcapsules. Self-activated samples were tested to failure and then healed by manual injection of DCPD monomer into the crack plane. This intermediate level control test enabled investigation of the embedded catalyst, without the variability of DCPD delivery through microencapsulation. The third type of sample was the fully self-contained, or *in situ*, system. *In situ* samples contained both the microencapsulated healing agent and Grubbs catalyst, enabling them to self-heal after fracture. Urea-formaldehyde microcapsules containing DCPD monomer were manufactured by an emulsion microencapsulation method outlined in White *et al.*³ Table 1 summarizes the different sample types.

Fracture specimens were tested under displacement control, using pin loading and a $5 \mu\text{m s}^{-1}$ displacement rate. Samples were tested to failure, measuring compliance and peak load. For the reference samples, 0.03 ml of pre-mixed DCPD monomer and Grubbs catalyst was injected into the crack plane, prior to crack closing. For the case of self-activated samples, 0.03 ml of DCPD monomer with no catalyst was injected into the crack plane, which was subsequently allowed to close. *In situ* samples were unloaded, allowing the crack faces to come back into contact. After a sufficient time for healing efficiency to reach a steady value, the healed samples were tested again. For the majority of experiments, the second test was performed after 48 h. Values of fracture toughness and the subsequent healing efficiency were calculated using eqs (2) and (5). A representative load-displacement curve is shown in Fig. 4 for the *in situ* healing case. The virgin fracture was brittle in nature, while the healed fracture exhibited prolonged stick-slip.

Healing of the Reference System

The healing system was first investigated via fracture toughness testing of reference samples. Following a virgin fracture test, approximately 0.03 ml of mixed DCPD monomer and catalyst was injected into the crack plane. An advantage of the ROMP healing system is the heterogeneous nature of the reaction. Unlike two part epoxy polymerization reactions, which require a precise stoichiometry ratio, the ROMP reaction can be triggered by discrete mixing at low concentration (10,000:1 monomer to catalyst ratio).

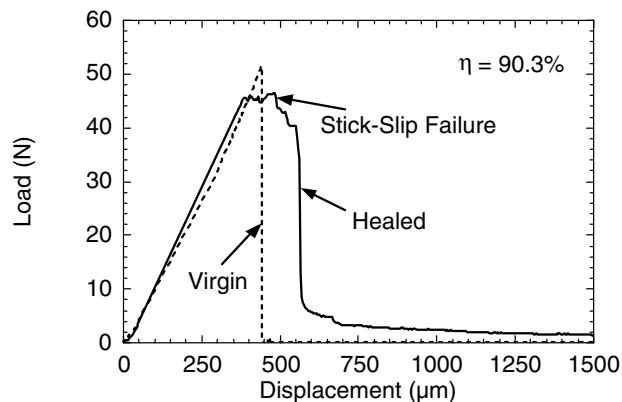


Fig. 4—Representative load-displacement curve for an *in situ* sample with 2.5 wt% Grubbs and 5 wt% microcapsules

Catalyst Concentration

The effect of the ratio of Grubbs catalyst to DCPD monomer was investigated by measuring the healing efficiency in four sets of samples with catalyst to DCPD ratios of 2, 4.4, 10 and 40 g liter^{-1} . Each set consisted of 18 samples. As shown in Table 2, the level of healing efficiency increased as the concentration of catalyst was increased, while the gel time decreased exponentially, taking approximately, 600, 235, 90 and 25 s, respectively.

An investigation of the fracture planes highlights two phenomena: fracture in pure epoxy results in locally smooth surfaces down to micrometer length scales (Fig. 5(a)) and fracture in the healed material occurs as separation between the bulk epoxy and polyDCPD film (Fig. 5(b)). The increased healing efficiency is attributed to changes in the chemical kinetics and thermodynamics with increased catalyst concentration. Shorter cure times reduce the time required for healing efficiency to reach a steady value and prevent diffusion and evaporation of DCPD from the crack plane. The ability of the healed reference sample to obtain full healing ($\eta = 100$ percent) indicates excellent adhesion between the polymerized DCPD and the epoxy.

Microcapsule Concentration

Reference samples have also been used to study the influence of microcapsule concentration on the fracture of the virgin and healed epoxy. Reference samples containing 0–25 percent by weight of microcapsules ($\sim 180 \mu\text{m}$ diameter) were tested to failure and healed manually. As observed earlier in the literature for the addition of solid particles,^{32,33} the virgin fracture toughness of the material increased significantly with increasing concentration of microcapsules, as shown in Fig. 6. A maximum was achieved at 15 wt% capsule concentration. Characteristic tails originating from broken spheres in the fracture plane (Fig. 5(c)) indicate a crack pinning toughening mechanism may be operative.

The healing agent released from the microcapsules was allowed to evaporate from the crack plane. The reference samples were then injected with a 4.4 g liter^{-1} mixture of Grubbs catalyst and DCPD monomer. The healed fracture toughness demonstrated minimal dependence on capsule concentration over a range of 5–20 percent by weight. For capsule

TABLE 1—SAMPLE TYPES

Sample Type	Epoxy (Epon 828:DETA)	Grubbs Catalyst	Microencapsulated Healing Agent
Reference control	100:12	—	0-25 %wt
Self-activated control	100:12	0.5 %wt	—
<i>In situ</i> self-healing	100:12	2.5 %wt	5-10 %wt

TABLE 2—INFLUENCE OF CATALYST CONCENTRATION ON HEALING EFFICIENCY IN REFERENCE SAMPLES

Concentration Grubbs (g):DCPD (l)	Fracture Toughness (MPa m ^{1/2})		Healing Efficiency
	Virgin	Healed	
40:1	0.55 ± 0.05	0.71 ± 0.08	Full heal
10:1	0.56 ± 0.04	0.61 ± 0.09	Full heal
4.4:1	0.55 ± 0.05	0.53 ± 0.10	97 ± 15%
2:1	0.54 ± 0.04	0.45 ± 0.08	84 ± 8%

concentrations close to the value that yields a maximum for the virgin fracture toughness (~15 wt%), a local minimum in healing efficiency occurred due to the minimal gains in healed fracture toughness, illustrated in Fig. 7. For a capsule concentration of 25 wt% and greater, near perfect healing was obtained. However, as the capsule concentration increased, the manufacture of samples was more difficult due to the increased viscosity of the uncured resin.

Healing of the Self-Activated System

The Grubbs catalyst is a fine purple powder with a propensity to form small clumps. Chemical investigation of the interactions between the catalyst and the epoxy system indicates that contact of the catalyst with the DETA curing agent can degrade the catalyst during manufacture.³⁴ The availability of active catalyst is dependent on the order of mixing the catalyst, resin and curing agent, the catalyst particle size, and the amount of catalyst added. These parameters are investigated with self-activated samples.

Mixing Order

The stability of the Grubbs catalyst in the current healing system was investigated previously using proton nuclear magnetic resonance (NMR)³⁴ (a standard technique for probing chemical structures³⁵). Although the Grubbs catalyst retained activity in the presence of the EPON[®] 828/DETA system during cure, contact with the DETA curing agent alone caused rapid deactivation of the catalyst. To ascertain the optimal mixing sequence of the three components (EPON[®] 828/12pph DETA/2.5 wt% Grubbs catalyst) for maximum catalyst activity and healing efficiency, six self-activated samples were manufactured for each of the three possible sequences. In each case, the first two components were mixed and degassed for 5 min. The third component was then integrated and degassed for an additional 5 min.

Fracture test results for the different mixing sequences are summarized in Table 3. Although virgin fracture toughness values are statistically unchanged, the healed fracture toughness values and in turn the efficiency of healing indicate the importance of mixing order. Mixing the catalyst and DETA curing agent first results in no measurable healing. Failure to recover fracture toughness indicates that the catalyst was extensively deactivated. The other two mixing orders had little effect on the healing efficiency.

Catalyst Particle Size

The size of the Grubbs catalyst particles also influenced the behavior of the virgin and healed composites. To determine the size distribution of the catalyst for maximum healing efficiency, a sample of catalyst was ground to provide a powder with particle diameters of less than 1 mm. Sets of six self-activated samples were manufactured with 2.5 wt% of catalyst with distributions of particle sizes of less than 75 μm, 75–180 μm, 180–355 μm and 355–1000 μm (Fig. 8). Both the virgin and healed fracture toughness values, plotted in Fig. 9, increased as the catalyst particle size increased. Poor healing efficiencies were obtained for small particles, due to low healed fracture toughness, and for large particles because the high healed fracture toughness was not coterminous with their high virgin fracture toughness. The highest healing efficiency corresponded to 180–355 μm catalyst particle size.

In the virgin material, the catalyst particles toughen through crack pinning,³⁶ as shown in Fig. 5(d). In the healed material, there are the competing effects of smaller particles providing improved dispersion—and thus availability of catalyst in the crack plane for polymerization of DCPD—and of larger particles providing a reduced surface area to volume ratio for the catalyst. The smaller surface area to volume ratio is believed to reduce the opportunity for DETA curing agent to react with the Grubbs catalyst.

Catalyst Concentration

To establish the catalyst concentration that provides for high healing efficiency without diminishing virgin fracture toughness, six sets of self-activated TDCB samples were manufactured with Grubbs catalyst concentrations from 0 wt% to 4 wt%. Each set consisted of six samples. Virgin and healed fracture toughness values and the corresponding healing efficiency have been measured and are plotted in Fig. 10. The healed fracture toughness increased with the addition of more catalyst. However, the relative gain in healed fracture toughness actually decreased for each additional increment of catalyst concentration. For a catalyst concentration beyond 3 wt%, the virgin fracture toughness decreased with further addition of catalyst. Although a high healing efficiency resulted at these high catalyst concentrations, gains were due to diminution of the virgin properties. Moreover, scatter in the data was dramatically increased at higher concentrations.

TABLE 3—INFLUENCE OF MIXING ORDER ON HEALING EFFICIENCY IN REFERENCE SAMPLES

Mixing Order	Fracture Toughness (MPa m ^{1/2})		Healing Efficiency
	Virgin	Healed	
(Epon 828 + DETA) + Grubbs	0.73 ± 0.06	0.45 ± 0.08	63 ± 6%
(Epon 828 + Grubbs) + DETA	0.75 ± 0.05	0.45 ± 0.09	60 ± 6%
(DETA + Grubbs) + Epon 828	0.76 ± 0.07	0	0%

Self-Healing of the In Situ System

The ultimate goal of this research was the development of a self-healing polymer composite. To achieve this, microencapsulated DCPD monomer and Grubbs catalyst were incorporated into an *in situ* sample. The effects of microcapsule size on healing efficiency and the evolution of healed fracture toughness over time were investigated using *in situ* samples with 2.5 wt% Grubbs catalyst and 10 wt% of DCPD monomer encapsulated microcapsules. The findings of these studies and the results presented thus far have been used to optimize the healing system through choice of catalyst and microcapsule concentration.

Microcapsule Size

Three sets of samples were manufactured with 180 ± 40 μm, 250 ± 80 μm and 460 ± 80 μm diameter capsules. When fracture occurred, DCPD monomer was observed to fill the crack plane of the TDCB specimen. Variation in the healed fracture toughness was small, with a trend for increased toughness with decreased capsule diameter as shown in Fig. 11. The divergence of healing efficiency was governed by the virgin fracture toughness, which increased significantly with decreased capsule diameter. The self-healed specimens with 460 μm diameter capsules exhibited the greatest healing efficiency, recovering 63 percent of virgin load on average. An investigation of the crack planes (Fig. 5(e)) revealed that all of the microcapsules fractured, releasing the encapsulated healing agent, with no mounds or protruding shell material representative of debonding.

Development of Healing Efficiency

The healing efficiencies presented thus far were measured after waiting 48 h after the virgin test. This time was chosen to ensure sufficient time for healing. Previous work with thermoplastics^{4–6} reported that healing efficiency was strongly tied to healing time. A series of 28 *in situ* samples was manufactured with 10 wt% of 180 μm diameter capsules and 2.5 wt% of catalyst. The virgin fracture tests were performed in rapid succession with the exact time of the fracture event noted for each specimen. Healed fracture tests were performed at time intervals ranging from 10 min to 72 h after the virgin test. The resulting healing efficiencies are plotted versus time in Fig. 12. A significant healing efficiency developed within 25 min, which closely corresponds to the gelation time of the polyDCPD. Steady-state values were reached within 10 h.

Microcapsule Concentration

In previous work on this self-healing system,^{3,37} microcapsule concentration was chosen to be 10 wt% to maximize DCPD delivery, while retaining near maximum virgin fracture toughness. For the large range of microcapsule sizes in-

vestigated in Fig. 11, only a small change in healed fracture toughness was measured. Excess DCPD was also observed during fracture for all capsule sizes. Moreover, the data for reference samples in Fig. 6 showed that a reduction in concentration from 10 wt% to 5 wt% had minimal impact on the healed fracture toughness. By reducing the capsule concentration, near perfect healing was obtained.

To investigate this effect for the self-healing case, a set of six *in situ* samples was manufactured with 5 wt% of 180 μm diameter capsules and 2.5 wt% of catalyst. An average healing efficiency of 85 ± 5% was measured. The relative healing efficiencies of neat epoxy and the *in situ* system with 10 wt% and 5 wt% microcapsules, are shown in Fig. 13, illustrating the successful development of an optimized self-healing system.

Conclusion

The use of TDCB fracture geometry has provided an accurate method to measure the fracture behavior and healing efficiency of self-healing polymer composites and to compare with appropriate controls. Virgin fracture properties of the polymer composite were improved by the inclusion of microcapsules and catalyst particles. The size and concentration of the catalyst were shown to have a significant impact on the virgin properties of the composite and the ability to catalyze the healing agent. The highest healing efficiency was obtained with 180–355 μm catalyst particles. Catalyst concentrations of greater than 2.5 wt% provided diminishing gains in healed fracture toughness. A significant loss of virgin fracture toughness was observed for a catalyst concentration of about 3%. The catalyst was found to remain active following the curing process, given that it was not first mixed with the DETA curing agent. The addition of microcapsules, up to 15 wt%, served to increase the virgin toughness. Capsule size had a direct influence on the volume of DCPD monomer released into the crack plane but, over the range of capsule sizes investigated, healing efficiency was not restricted by lack of healing agent. Maximum healing efficiency was obtained within 10 h of the fracture event. By optimizing the concentrations of catalyst and microcapsules, the healing efficiency of the system was increased to over 90 percent.

Acknowledgments

The authors gratefully acknowledge the support of the University of Illinois Critical Research Initiative Program, AFOSR Aerospace and Materials Science Directorate Mechanics and Materials Program, and Motorola Labs, Motorola Advanced Technology Center Schaumburg IL. Special thanks are extended to Dr A. Skipor of Motorola Labs for his continuing support and suggestions. The authors would also like to thank Prof. J.S. Moore, Prof. P.H. Geubelle and graduate students M.R. Kessler and S.R. Sriram for technical support and helpful discussions. Undergraduate B. Lung was

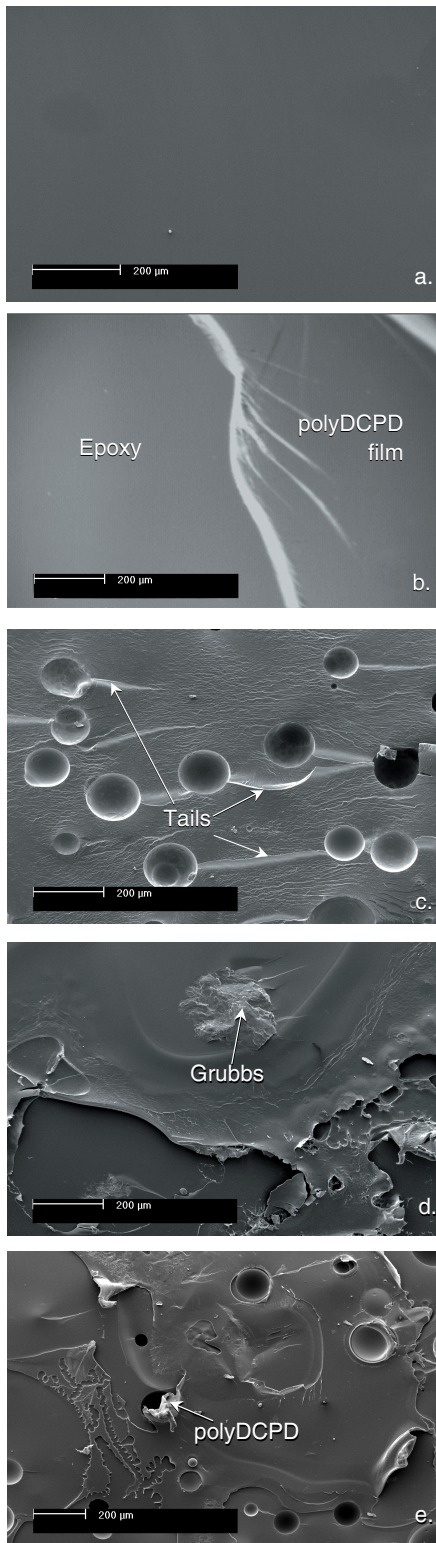


Fig. 5—Crack plane environmental scanning electron microscopy (ESEM) images: (a) neat epoxy; (b) polyDCPD separation from bulk epoxy; (c) reference sample (10 wt% capsules) showing tails related to the crack pinning toughening mechanism; (d) self-activated (2.5 wt% Grubbs catalyst); (e) *in situ* samples (10 wt% capsules and 2.5 wt% catalyst). The crack propagation direction is from left to right in all images

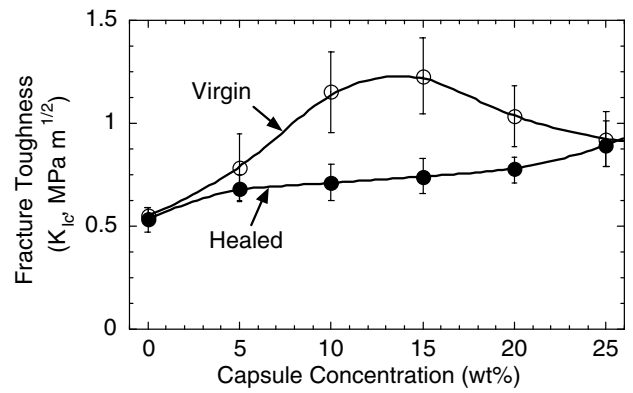


Fig. 6—Virgin and healed fracture toughness as a function of capsule concentration

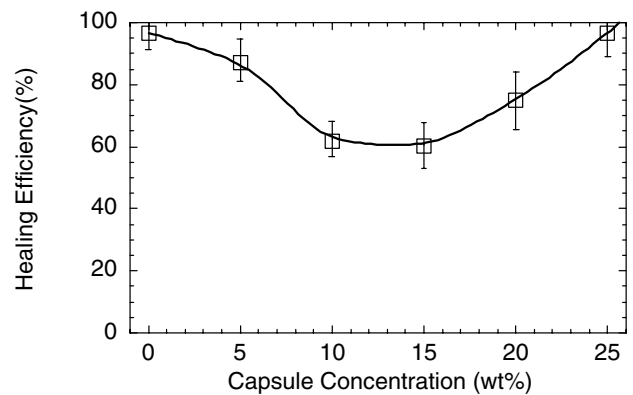


Fig. 7—Healing efficiency as a function of capsule concentration

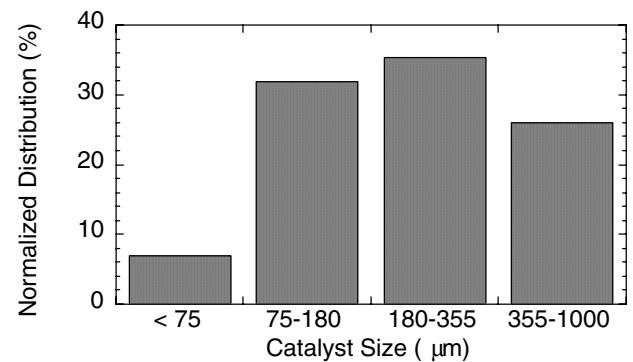


Fig. 8—Particle size distribution of the Grubbs catalyst following grinding

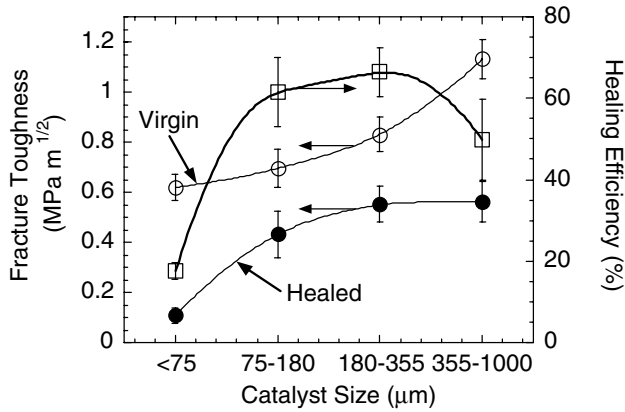


Fig. 9—The effect of catalyst particle size on fracture toughness and healing efficiency

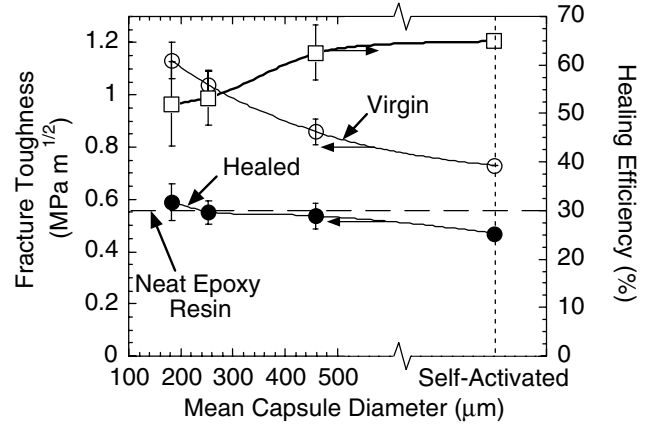


Fig. 11—Influence of microcapsule size on fracture toughness and healing efficiency

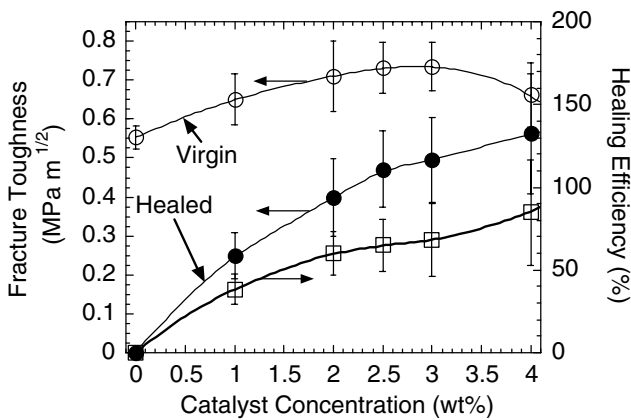


Fig. 10—Fracture toughness and healing efficiency as a function of catalyst concentration

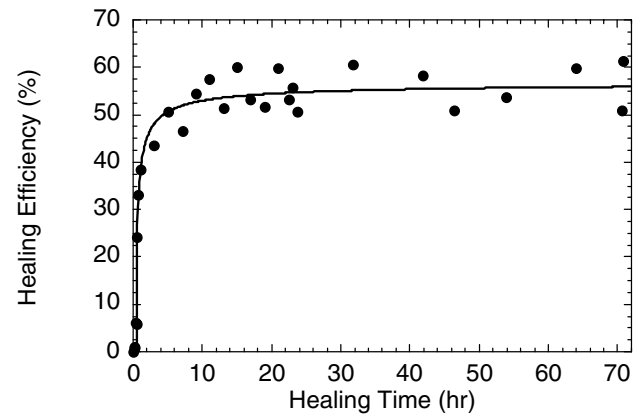


Fig. 12—Development of healing efficiency

extremely helpful in the preparation of the TDCB samples. Electron microscopy was performed in the Imaging Technology Group, Beckman Institute, of the University of Illinois, with the assistance of S. Robinson.

References

1. Caplan, A.I., "Bone Development, Cell and Molecular Biology of Vertebrate Hard Tissues," Ciba Foundation Symposium, **136**, 3–16, John Wiley & Sons (1988).
2. Albert, S.F., "Electrical Stimulation of Bone Repair," Clin. Podiatric Med. Surg., **8**, 923–935 (1981).
3. White, S.R., Sottos, N.R., Geubelle, P.H., Moore, J.S., Kessler, M.R., Sriram, S.R., Brown, E.N., and Viswanathan, S., "Autonomic Healing of Polymer Composites," Nature, **409**, 794–797 (2001).
4. Wool, R.P., and O'Conner, K.M., "A Theory of Crack Healing in Polymers," J. Appl. Phys., **52**, 5953–5963 (1982).
5. Jud, K., and Kausch, H.H., "Load Transfer Through Chain Molecules After Interpenetration at Interfaces," Polym. Bull., **1**, 697–707 (1979).
6. Kausch, H.H., and Jud, K., "Molecular Aspects of Crack Formation and Healing in Glassy Polymers," Rubber Process. Appl., **2**, 265–268 (1982).
7. Sukhotskaya, S.S., Mazhorava, V.P., and Terekhin, Yu N., "Effect of Autogenous Healing of Concrete Subjected to Periodic Freeze Thaw," Hydrotech. Constr., **17**, 295–296 (1983).
8. Clear, C.A., "The Effect of Autogenous Healing upon Leakage of Water through Cracks in Concrete," Cement and Concrete Association, Wexham Spring, May (1985).
9. Edvardsen, C., "Water Permeability and Autogenous Healing of Cracks in Concrete," ACI Mater. J., **96**, 448–454 (1999).

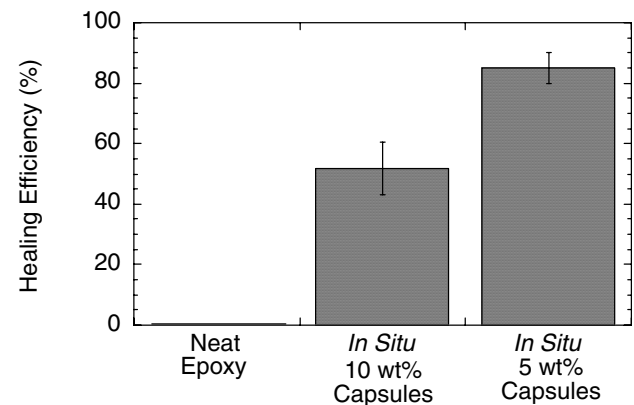


Fig. 13—Comparison of *in situ* healing efficiency for different capsule concentrations (2.5 wt% catalyst)

10. Kim, Y.R., and Little, D., "Evaluation of Self-Healing in Asphalt Concrete by Means of the Theory of Nonlinear Elasticity," Transp. Res. Rec., no. 1228, 198–210 (1989).
11. Stavridis, B., and Holloway, D.G., "Crack Healing in Glass," Phys. Chem. Glasses, **24**, 19–25 (1983).
12. Jung, D., "Performance and Properties of Embedded Microspheres for Self-Repairing Applications," MS Thesis, University of Illinois at Urbana-Champaign (1997).

13. Hegeman, A., "Self-repairing Polymers, Repair Mechanisms and Micromechanical Modeling," MS Thesis, University of Illinois at Urbana-Champaign (1997).
14. Jung, D., Hegeman, A., Sottos, N.R., Geubelle, P.H., and White, S.R., "Self-healing Composites Using Embedded Microspheres," *Proc. American Society for Mechanical Engineers (ASME), Symposium on Composites and Functionally Graded Materials*, Dallas, TX, eds. K. Jacob, N. Katsube and W. Jones, ASME, MD-80, 265–275 (1997).
15. Zako, M., and Takano, N., "Intelligent Material Systems Using Epoxy Particles to Repair Microcracks and Delamination Damage in GFRP," *J. Intell. Mater. Syst. Struct.*, **10**, 836–841 (1999).
16. Wiederhorn, S.M., and Townsend, P.R., "Crack Healing in Glass," *J. Am. Ceram. Soc.*, **53**, 486–489 (1970).
17. Inagaki, M., Urashima, K., Toyomasu, S., Goto, Y., and Sakai, M., "Work of Fracture and Crack Healing in Glass," *J. Am. Ceram. Soc.*, **68**, 704–706 (1985).
18. Jud, K., Kausch, H. H., and Williams, J. G., "Fracture Mechanics Studies of Crack Healing and Welding of Polymers," *J. Mater. Sci.*, **16**, 204–210 (1981).
19. Wang, P.P., Lee, S., and Harmon, J.P., "Ethanol-induced Crack Healing in Poly(methyl methacrylate)," *J. Polym. Sci., B*, **32**, 1217–1227 (1994).
20. Lin, C.B., Lee, S.B., and Liu, K.S., "Methanol-Induced Crack Healing In Poly(Methyl Methacrylate)," *Polym. Eng. Sci.*, **30**, 1399–1406 (1990).
21. Raghavan, J., and Wool, R.P., "Interfaces in Repair; Recycling Joining and Manufacturing of Polymers and Polymer Composites," *J. Appl. Polym. Sci.*, **71**, 775–785 (1999).
22. Wool, R.P., "Polymer Interfaces: Structure and Strength," Ch. 12, 445–479, Hanser Gardner, Cincinnati (1995).
23. Dry, C., "Procedures Developed for Self-repair of Polymeric Matrix Composite Materials," *Compos. Struct.*, **35**, 263–269 (1996).
24. Motuku, M., Vaidya, U.K., and Janowski, G.M., "Parametric Studies on Self-repairing Approaches for Resin Infusion Composites Subjected to Low Velocity Impact," *Smart Mater. Struct.*, **8**, 623–638 (1999).
25. Li, V.C., Lim, Y.M., and Chan, Y., "Feasibility Study of a Passive smart Self-healing Cementitious Composite," *Composites B*, **29B**, 819–827 (1998).
26. Mostovoy, S., Crosley P.B., and Ripling, E.J., "Use of Crack-Line Loaded Specimens for measuring Plain-Strain Fracture Toughness," *J. Mater.*, **2**, 661–681 (1967).
27. Irwin, G.R., and Kies, J.A., "Critical Energy Rate Analysis of Fracture Strength," *Am. Welding Soc. J.*, **33**, 193-s–198-s (1954).
28. Beres, W., Ashok, K.K., and Thambraj, R., "A Tapered Double-Cantilever-Beam Specimen Designed for Constant-K Testing at Elevated Temperatures," *J. Test. Eval.*, **25**, 536–542 (1997).
29. Meiller, M., Rocje, A.A., and Sautereau, H., "Tapered Double-Cantilever-Beam Test Used as a Practical Adhesion Test for Metal/Adhesive/Metal Systems," *J. Adhes. Sci.*, **13**, 773–788 (1999).
30. Marcus, H.L., and Sih, G.C., "A Crackline-Loaded Edge-Crack Stress Corrosion Specimen," *Eng. Fracture Mech.*, **3**, 453–461 (1971).
31. Freed, C.N., and Kraft, J.M., "Effect of Side Grooving on Measurements of Plain Strain Fracture Toughness," *J. Mater.*, **1**, 770–790 (1966).
32. Evans, A.G., "The Strength of Brittle Materials Containing Second Phase Dispersions," *Phil. Mag.*, **26**, 1327–1344 (1972).
33. Broutman, L.J., and Sahu, S., "The Effect of Interfacial Bonding on the Toughness of Glass Filled Polymers," *Mater. Sci. Eng.*, **8**, 98–107 (1971).
34. Sriram, S., "Development of Self-healing Polymer Composites and Photoinduced Ring Opening Metathesis Polymerization," PhD Thesis, University of Illinois at Urbana-Champaign (2002).
35. Ulman, M., and Grubbs, R.H., "Ruthenium Carbene-based Olefin Metathesis Initiators: Catalyst Decomposition and Longevity," *J. Org. Chem.*, **64**, 7202–7207 (1999).
36. Lange, F.F., "The Interaction of a Crack Front with a Second-phase Dispersion," *Phil. Mag.*, **22**, 983–992 (1970).
37. Brown, E.N., and Sottos, N.R., "Performance of Embedded Microspheres for Self-Healing Polymer Composites," *Society for Experimental Mechanics IX International Congress on Experimental Mechanics*, 563–566 (2000).